

## DAEMONFLUX: Data-Driven Muon-Calibrated Neutrino Flux

Anatoli Fedynitch<sup>a,b,\*</sup> and Juan Pablo Yañez<sup>c</sup>

<sup>a</sup>*Institute of Physics, Academia Sinica, Taipei City, 11529, Taiwan*

<sup>b</sup>*Institute for Cosmic Ray Research, the University of Tokyo, 5-1-5 Kashiwa-no-ha, Kashiwa, Chiba 277-8582, Japan*

<sup>c</sup>*Dept. of Physics, University of Alberta  
Edmonton, Alberta, Canada T6G 2E1*

E-mail: [anatoli@gate.sinica.edu.tw](mailto:anatoli@gate.sinica.edu.tw)

This study presents a refined calculation of the atmospheric neutrino flux from GeV to PeV energies based on two data-driven models for the flux of cosmic ray nucleons (GSF6) and hadronic interactions (DDM, previously detailed in [1]). The uncertainties are treated as adjustable parameters and are fitted using a combination of muon spectrometer data at the surface, including constraints from fixed-target experiments. The resulting calculated neutrino fluxes have uncertainties of less than 10% up to 1 TeV and show significant differences compared to previous calculations. We discuss which experiments have the most significant impact on the fit and propose how this method can incorporate additional constraints, such as measurements of deep underground muon intensities or seasonal variations, in the future. Our model is publicly available via the DAEMONFLUX code, which provides access to all model parameters and the covariance matrix obtained from the fit.

38th International Cosmic Ray Conference (ICRC2023)  
26 July - 3 August, 2023  
Nagoya, Japan



---

\*Speaker

## 1. Introduction

Atmospheric neutrinos are a product of the hadronic component of particle showers triggered by cosmic rays interacting with Earth's atmosphere. The majority of these neutrinos are produced as a result of the decay of  $\pi$  and  $K$  mesons, which also give rise to muons. Some of these muons will undergo decay in flight, producing additional neutrinos in the process.

One major source of uncertainty for the computation of neutrino fluxes comes from the limited knowledge of the primary cosmic rays that initiate the atmospheric showers [2]. Historically the primary cosmic ray flux has been modeled as a collection of multiple nuclei that follow a power-law spectrum, fitting the scaling factor and spectral index to data from multiple experiments that were not always in agreement [3]. The other main uncertainty in flux calculations comes from the phase space of hadronic interactions that is relevant for the observed neutrinos, namely light meson production at very small scattering angles [4]. Phenomenological models of hadronic interactions, such as SIBYLL-2.3D [5, 6], are commonly used as an alternative. However, accurately modeling forward particle distributions in the relevant phase space requires comparing these models to data obtained from fixed-target experiments, which are typically not conducted at TeV energies and do not cover sufficient phase space. One way to minimize these uncertainties is to utilize the correlation between the flux of atmospheric neutrinos and that of cosmic muons, which originate from the same decay of charged mesons and are comparatively easier to detect and characterize [7].

In this work we exploit the muon-neutrino relationship, extending it to include flux and muon charge ratio measurements from multiple experiments. The result is DAEMONFLUX<sup>1</sup> [8], a *calibrated* atmospheric neutrino flux with a covariance matrix of well defined uncertainties, presented in extensive detail in Ref. [9].

## 2. Modeling Atmospheric Muon and Neutrino Fluxes

For this work we compute inclusive atmospheric lepton fluxes at energies above a few GeV using one-dimensional coupled cascade equations. To solve the cascade equations we employ the code MCEQ 1.4<sup>2</sup> [1, 6, 10], which numerically solves for the evolution of particle densities as they propagate through a gaseous or dense medium. As hadronic interaction model, we use the Data-Driven hadronic interaction Model (DDM) [1], which is specifically designed for lepton flux calculations and comes with advantages for this particular work. DDM contains parameterization of cross sections and their uncertainties obtained from the data of the NA49 and NA61 fixed target experiments. The numerical representations have adjustable parameters with error bounds that can be used as fit parameters in the muon calibration.

To implement a viable model of the cosmic ray nucleon fluxes (see Figure 1 (left)), we created a specialized version of the Global Spline Fit [11]. This model is a parametric spline representation of the all particle cosmic ray spectrum and of individual mass groups, hence it contains over 80 free parameters fit to data. However, the nucleon fluxes (in the basis of energy per nucleon) are dominated by only two components, protons and helium. Therefore, there must exist a simpler model with fewer parameters that represents all relevant features and the variance of the model.

<sup>1</sup><https://github.com/mceq-project/daemonflux>

<sup>2</sup><https://github.com/mceq-project/MCEq>

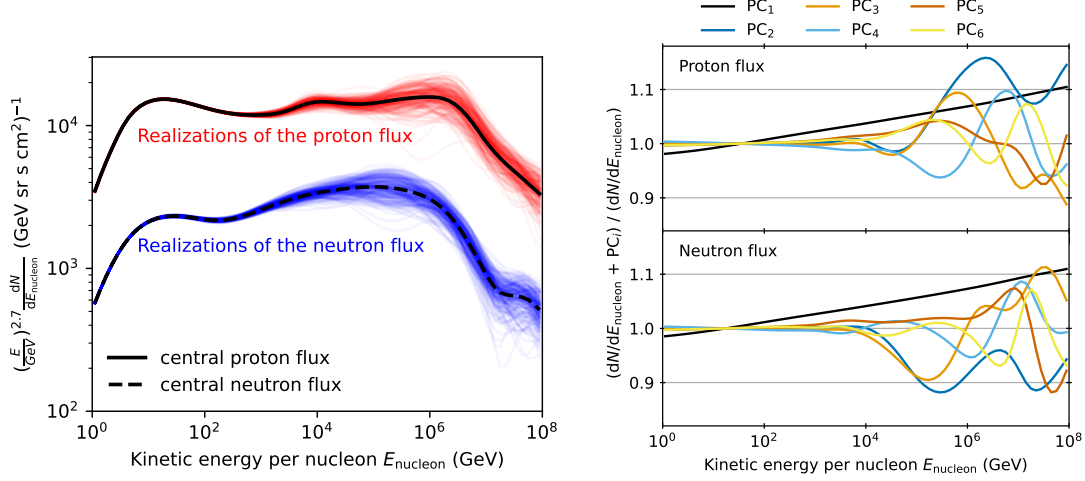


**Figure 1:** (left) Simulated variations of the proton and neutron fluxes based on the uncertainties of the GSF model. These realizations were generated using the covariance matrix of the model’s parameters. At energies above 10 TeV, the model exhibits increased spread due to the limited precision of direct cosmic ray experiments and the absence of reliable indirect data that is sensitive to composition. (right) Spectral features of the six PCs of GSF-PCA6. The panels show the ratio of the total nucleon fluxes, where each component is modified by  $+1\sigma$ . The leading component,  $PC_1$ , is a uniform spectral index correction for proton and neutron fluxes. Other PCs show (anti-)correlations between proton and neutron, that physically originate from fitting the all-particle and elemental spectra within the GSF approach. At energies of the knee, the other PCs significantly deviate from a power-law spectrum, indicating that a further simplification of the cosmic ray flux errors requires careful assessment.

We employ the Principal Component Analysis (PCA), a statistical method for reducing the complexity of a dataset. The goal is to transform the data into a new coordinate system, where the covariance matrix of the new parameters, referred to as the principal components (PCs), is diagonal. Aiming to capture  $\sim 90\%$  of the full model’s variance, we choose six PCAs and call the model GSF-PCA6 (more detailed discussion in Ref. [9]). Figure 1 demonstrates the variation of the nucleon fluxes by varying the PCAs by  $1\sigma$ . It is remarkable that the dominant component returned mathematically by the method is a simple variation of the spectral index, which is a typical nuisance parameter widely applied in data analyses.

We propagate the errors of the DDM and the GSF-PCA6 model to atmospheric lepton fluxes using linear error propagation based on gradients with respect to hadronic and cosmic ray parameters  $\mathcal{P}$  by perturbing secondary particle yields ( $dN^{\mathcal{P}}/dx_{\text{Lab}}$ ) and the principal components, respectively:

$$\delta\Phi_{\mu}(E_{\mu})_{\mathcal{P}} = \frac{\Phi_{\mu}(E_{\mu}, (1 + \delta)\frac{dN^{\mathcal{P}}}{dx_{\text{Lab}}}) - \Phi_{\mu}(E_{\mu}, (1 - \delta)\frac{dN^{\mathcal{P}}}{dx_{\text{Lab}}})}{2\delta}. \quad (1)$$

An equivalent  $1\sigma$  scale for the  $\mathcal{P}$ -parameters is derived by equalizing the errors of spectrum-weighted moments (Z-factors) between this scheme and a more rigorous approach shown in [9]:

$$\delta Z_{\mathcal{P}D_i} \equiv \mathcal{P}_i \int_0^1 dx_{\text{Lab}} x^{1.7} \frac{dN^{\mathcal{P}}}{dx_{\text{Lab}}}. \quad (2)$$

The Z-factor error  $\delta Z_{p\mathcal{D}_i}$  is calculated from the DDM splines by standard error propagation. This approach ensures that  $\mathcal{P}_i = \pm 1$  approximately corresponds to  $\mathcal{D} = \pm 1$ , which is the propagated  $1\sigma$  error of the accelerator data.

The hadronic yields in the DDM are assumed to follow Feynman scaling. However, to increase flexibility at projectile energies  $E_p > 158$  GeV, additional parameters are introduced as part of this work. This is done by “cloning” the 158 GeV yields ( $dN/dx_{\text{Lab}}$ ) at higher projectile energies and linearly interpolating between these points in  $\log E_p$ . These additional degrees of freedom allow us to test potential deviations from Feynman scaling and quantify the extrapolation errors of the muon and neutrino fluxes above TeV energies. We assessed the effect of adding parameters for all particle yields at 2 TeV, 20 TeV, 200 TeV, and 2 PeV on the muon flux and charge ratio predictions. Our results revealed that a gap of at least two decades in energy was necessary to prevent strong correlations. The majority of sensitivity was found to be in the pion yields, while variations in other particles had a limited impact on the muon flux. As a result, we retained two additional calibration points for pions at 20 TeV and 2 PeV, and one point at 2 PeV for the rest of the hadronic yields.

### 3. Selection of muon datasets and fitting

We surveyed the literature to collect all published measurements of muon fluxes and charge ratios by spectrometers as a function of energy or momentum, and studied the subset with muon momentum higher than 5 GeV at the detector to avoid complications introduced by geomagnetic effects, not yet included in MCEq. Our survey included the comprehensive list of historical measurements presented in [12] as well as the modern measurements reported in [13]. After performing data-data compatibility tests and considerations we retain only the 7 datasets listed in Table 1 of Ref. [9]. A key aspect of our fit procedure is that, whenever possible, we account for the systematic uncertainties of each experiment by introducing correction functions that modify the reported measurements. We were able to do this for BESS-TeV, L3+c and MINOS. We note that these corrections are necessary to bring the vertical fluxes of BESS-TeV and L3+c into agreement.

The calibration of the lepton fluxes is done by fitting the muon fluxes and the  $R_{\mu^+/\mu^-}$  produced by MCEq to data by varying 34 parameters: six from the GSF-PCA6 model, 18 from the DDM including the extrapolation parameters, and 10 are corrections to the experimental uncertainties of the data in the fit. The test statistic is a modified  $\chi^2$  given by

$$\chi^2 = \sum_i^N \frac{(O_i - T_i)^2}{\sigma_{O_i}^2} + \sum_j^M \frac{(F_j - G_j)^2}{\sigma_{F_j}^2} \quad (3)$$

where the first sum compares observation  $O_i$  at each data point  $i$  with expectation  $T_i$  from MCEq divided by the error in the observation  $\sigma_{O_i}$ . The second sum accounts for prior knowledge on each  $M$  parameter, penalizing deviations  $F_j$  from their expectation  $G_j$  divided by its estimated error  $\sigma_{F_j}$ . At each iteration of the fit, all experimental data sets are modified and the expectation is recomputed.

### 4. Results

After performing the fit to muon data, we estimate the agreement between data and our model by computing a  $\chi^2$  (using only the first term of Eq. 3), and obtained a value of 199 with approximately

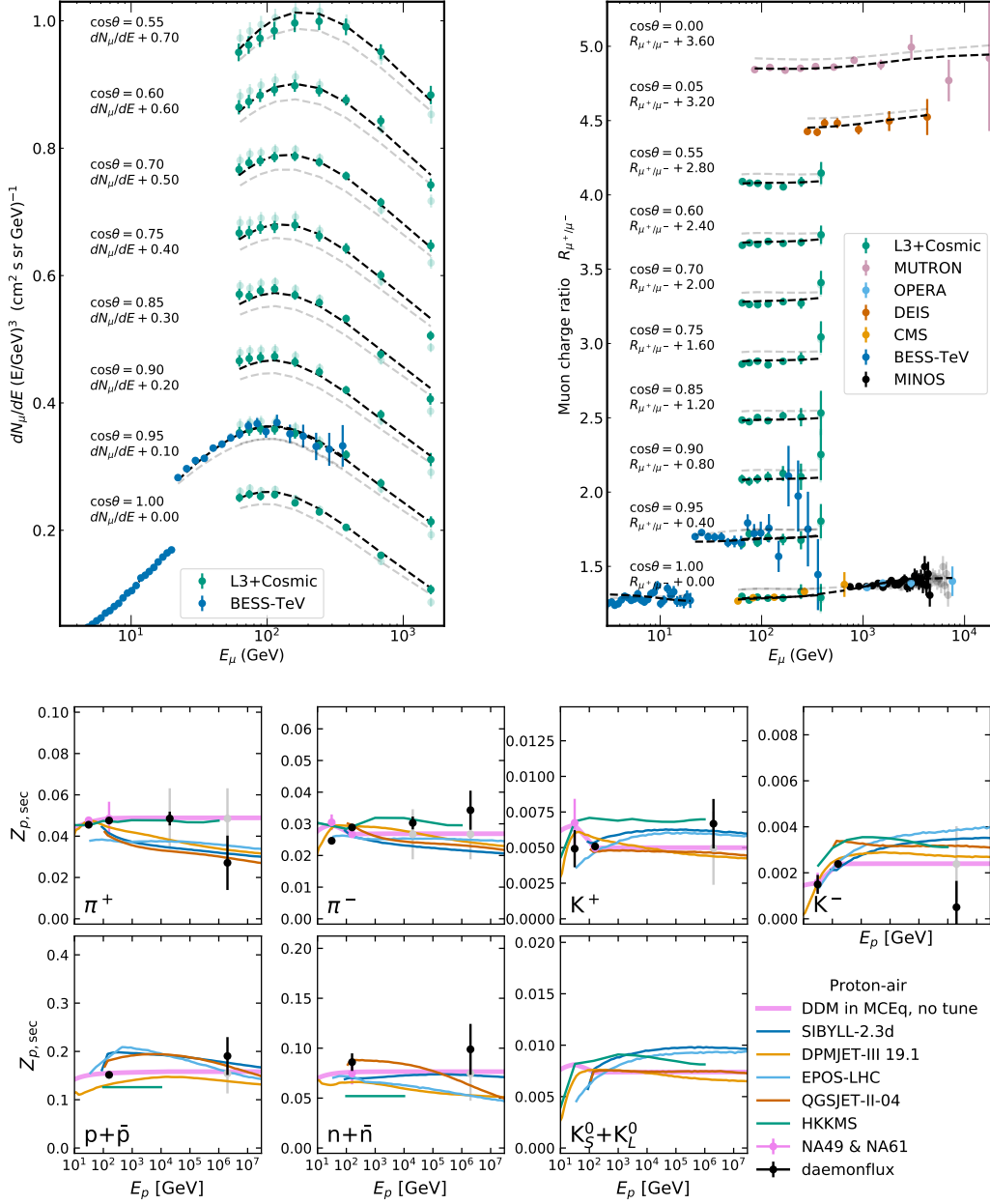


**Figure 2:** Muon fluxes for near vertical incoming directions (top left) and muon charge ratio for all data used in the fit (top right). Solid colors correspond to the experimental data and the flux calculation after the fit. The data and predictions prior to the fit are shown with a transparency. A factor has been added to fluxes from different incoming directions to be able to show them in the same figures.

Spectrum-weighted moments (Z-factors) shown as a function of energy for air target (bottom panel). They were computed assuming an incoming spectral index  $\gamma = 1.7$  following Eq. 2. The result of this work is labeled **DAEMONFLUX** and is shown in black. The grey points, located at the same energies (if visible) correspond to the starting value and uncertainty prior to the fit. Shown for comparison are the corresponding Z-factors from the DDM, HKKMS, DPMJet, Sibyll, QGSJET and EPOS-LHC [14–17]. Uncertainties for the  $\star$ -parameters are estimated from the spread of these models.

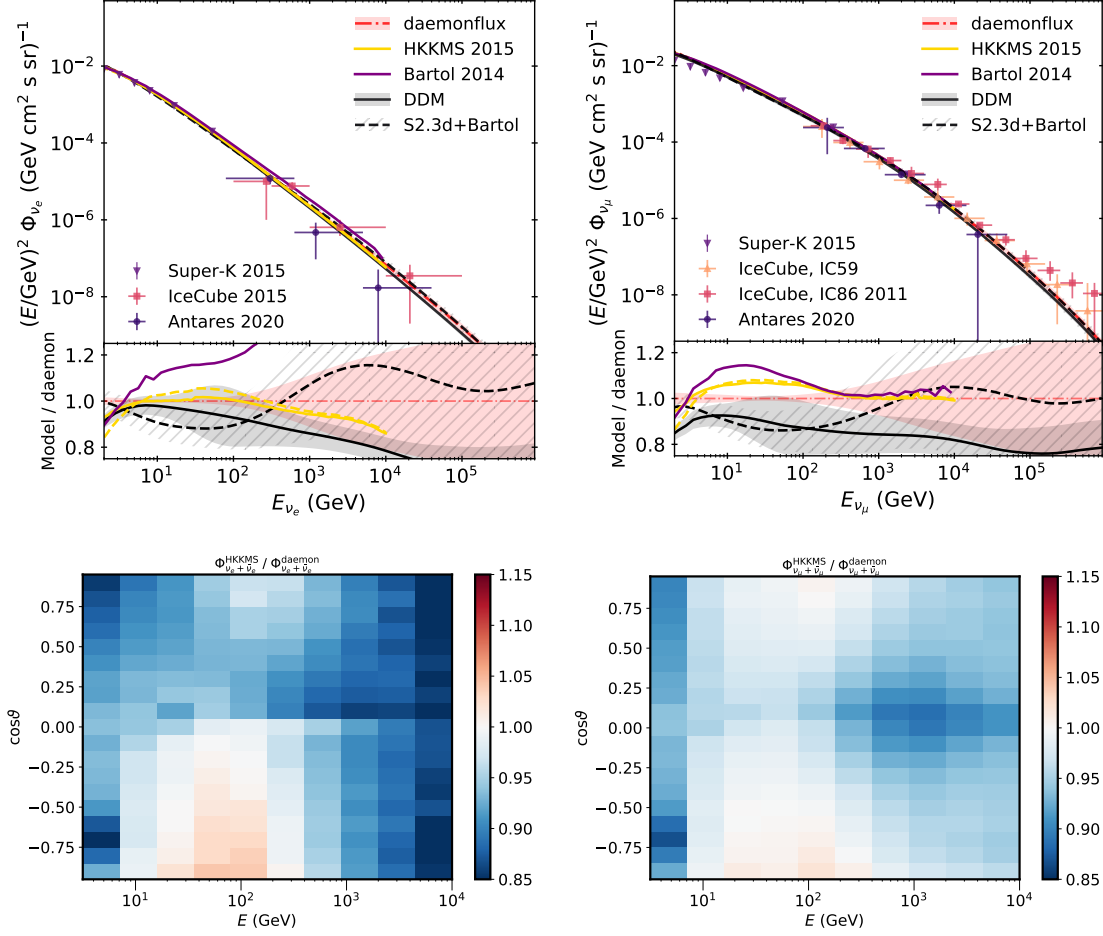


**Figure 3:** top: Conventional atmospheric electron neutrino (left) and muon neutrino (right) fluxes averaged over zenith angles shown together with data from Super-Kamiokande, IceCube, and ANTARES (see [9] for references). bottom: Ratio of flux of electron and muon neutrinos and antineutrinos from the prediction from Honda et al and our calculation. The fluxes were scaled to the same value at  $E_\nu = 25$  GeV and  $\cos \theta = -0.5$  to highlight their shape difference.

217 degrees of freedom. The number of degrees of freedom was estimated as number of data points minus the number of free parameters in the fit. This results in a  $p$ -value of 81%, indicating excellent agreement between the corrected data and the corrected model.

The muon fluxes and muon charge ratios obtained from the analysis can be seen in Fig. 2, which show the muon measurement data and the prediction from the model before and after the fit. The figure also shows the impact of the correction functions on experimental data. Prior to the fit, the prediction from GSF+DDM is in significant tension with the data, both for flux and charge ratio. After the fit is performed, and the data is corrected, the muon flux calculations can describe the data sets over the entire parameter space. The lower panel of Figure 2 shows the results for hadronic yields as  $Z$ -factors, in comparison with predictions from multiple hadronic interaction models. Most of the resulting hadronic yields are near to one of the models tested, although none of the existing models follows the trend in energy of our result over all the yields. The assumption

of scaling used in the DDM is significantly violated by the pion results, while for the kaons and baryons the error bars are large enough to be compatible with it.

The atmospheric neutrino fluxes after muon calibration are displayed in Fig 3, along with predictions from various models and experimental data. Our result displays interesting differences from the HKMS 2015 model, which has been used to interpret atmospheric neutrino data below 1 TeV by various experiments (see e.g. [18, 19]). For  $\nu_e$ , our calculation predicts a flux about 5% lower between  $\sim 40 - 1000$  GeV, with the difference growing with energy. For  $\nu_\mu$  the discrepancy between both models is closer to 8% between  $\sim 5 - 100$  GeV, then agreeing for higher energies.

## 5. Conclusion

The DAEMONFLUX atmospheric lepton flux model represents a significant departure from previous methods of calculating fluxes and characterizing their uncertainties. By incorporating data-driven models for the cosmic ray spectrum (GSF6) and secondary particle yields (DDM) into an accurate cascade equation solver (MCEq), we can propagate the uncertainties of these models to the prediction of atmospheric muon fluxes, which are closely related to atmospheric neutrino fluxes. Using precise spectrometer data of muon fluxes at the surface, we developed a fitting framework that uses corrections to the initial model uncertainties as fit parameters to produce a best fit and a fully data-driven estimate of uncertainties. The result is a flux model with the lowest uncertainties to date, reducing them by dozens of percent in energy ranges where relevant muon data is available.

In future iterations, we will employ the code MUTE [20, 21] to further constrain its parameters using a selection of muon measurements underground. In the contribution [21], we present that the underground data is well described by the present DAEMONFLUX.

## References

- [1] A. Fedynitch and M. Huber, *Data-driven hadronic interaction model for atmospheric lepton flux calculations*, *Phys. Rev. D* **106** (2022) 083018 [[2205.14766](#)].
- [2] J. Evans, D.G. Gamez, S.D. Porzio, S. Söldner-Rembold and S. Wren, *Uncertainties in Atmospheric Muon-Neutrino Fluxes Arising from Cosmic-Ray Primaries*, *Phys. Rev. D* **95** (2017) 023012 [[1612.03219](#)].
- [3] T.K. Gaisser and M. Honda, *Flux of atmospheric neutrinos*, *Ann. Rev. Nucl. Part. Sci.* **52** (2002) 153 [[hep-ph/0203272](#)].
- [4] G.D. Barr, T.K. Gaisser, S. Robbins and T. Stanev, *Uncertainties in Atmospheric Neutrino Fluxes*, *Phys. Rev. D* **74** (2006) 094009 [[astro-ph/0611266](#)].
- [5] F. Riehn, R. Engel, A. Fedynitch, T.K. Gaisser and T. Stanev, *Hadronic interaction model Sibyll 2.3d and extensive air showers*, *Phys. Rev. D* **102** (2020) 063002 [[1912.03300](#)].
- [6] A. Fedynitch, F. Riehn, R. Engel, T.K. Gaisser and T. Stanev, *Hadronic interaction model sibyll 2.3c and inclusive lepton fluxes*, *Phys. Rev. D* **100** (2019) 103018 [[1806.04140](#)].



- [7] M. Honda, T. Kajita, K. Kasahara, S. Midorikawa and T. Sanuki, *Calculation of atmospheric neutrino flux using the interaction model calibrated with atmospheric muon data*, *Phys. Rev. D* **75** (2007) 043006 [[astro-ph/0611418](#)].
- [8] A. Fedynitch and J.P. Yanez, *daemonflux 0.7.0*, Jun, 2023. [10.5281/zenodo.7994523](#).
- [9] J.P. Yañez and A. Fedynitch, *Data-driven muon-calibrated neutrino flux*, *Phys. Rev. D* **107** (2023) 123037 [[2303.00022](#)].
- [10] A. Fedynitch, R. Engel, T.K. Gaisser, F. Riehn and T. Stanev, *Calculation of conventional and prompt lepton fluxes at very high energy*, *EPJ Web Conf.* **99** (2015) 08001 [[1503.00544](#)].
- [11] H.P. Dembinski, R. Engel, A. Fedynitch, T. Gaisser, F. Riehn and T. Stanev, *Data-driven model of the cosmic-ray flux and mass composition from 10 GeV to 10<sup>11</sup> GeV*, *PoS ICRC2017* (2018) 533 [[1711.11432](#)].
- [12] G. Fiorentini, V.A. Naumov and F.L. Villante, *Atmospheric neutrino flux supported by recent muon experiments*, *Phys. Lett. B* **510** (2001) 173 [[hep-ph/0103322](#)].
- [13] PARTICLE DATA GROUP collaboration, *Review of Particle Physics*, *PTEP* **2022** (2022) 083C01.
- [14] S. Roesler, R. Engel and J. Ranft, *The monte carlo event generator dpmjet-iii*, in *Advanced Monte Carlo for radiation physics, particle transport simulation and applications.*, pp. 1033–1038, 2001, DOI [[hep-ph/0012252](#)].
- [15] A. Fedynitch, *Cascade equations and hadronic interactions at very high energies*, Ph.D. thesis, KIT, Karlsruhe, Dept. Phys., 11, 2015. [10.5445/IR/1000055433](#).
- [16] S. Ostapchenko, *Monte Carlo treatment of hadronic interactions in enhanced Pomeron scheme: I. QGSJET-II model*, *Phys. Rev. D* **83** (2011) 014018 [[1010.1869](#)].
- [17] T. Pierog, I. Karpenko, J.M. Katzy, E. Yatsenko and K. Werner, *EPOS LHC: Test of collective hadronization with data measured at the CERN Large Hadron Collider*, *Phys. Rev. C* **92** (2015) 034906 [[1306.0121](#)].
- [18] SUPER-KAMIOKANDE collaboration, *Atmospheric Neutrino Oscillation Analysis with Improved Event Reconstruction in Super-Kamiokande IV*, *PTEP* **2019** (2019) 053F01 [[1901.03230](#)].
- [19] ICECUBE collaboration, *All-flavor constraints on nonstandard neutrino interactions and generalized matter potential with three years of IceCube DeepCore data*, *Phys. Rev. D* **104** (2021) 072006 [[2106.07755](#)].
- [20] A. Fedynitch, W. Woodley and M.-C. Piro, *On the Accuracy of Underground Muon Intensity Calculations*, *Astrophys. J.* **928** (2022) 27 [[2109.11559](#)].
- [21] W. Woodley, A. Fedynitch and M.-C. Piro, *Challenges and Opportunities for Predicting Muons in Underground and Underwater Labs Using MUTE*, *PoS ICRC2023* (2023) tba.